A Section 508–conformant HTML version of this article is available at https://doi.org/10.1289/EHP10273.

Screening of Organophosphate Flame Retardants with Placentation-Disrupting Effects in Human Trophoblast Organoid Model and Characterization of Adverse Pregnancy Outcomes in Mice

Chenke Xu,[1] Haojia Ma,[1*] Fumei Gao,[2*] Chenhao Zhang,[1] Wenxin Hu,[1] Yingting Jia,[1] Jun Xu,[3] and Jianying Hu[1]*

[1]MOE Laboratory for Earth Surface Process, College of Urban and Environmental Sciences, Peking University, Beijing, China
[2]Reproductive Medical Center, Peking University People's Hospital, Peking University, Beijing, China
[3]Department of Cell Biology, School of Basic Medical Sciences, Peking University Stem Cell Research Center, Peking University Health Science Center, Peking University, Beijing, China

Background: Abnormal placental development may result in adverse pregnancy outcomes and metabolic diseases in adulthood; however, it remains unknown whether and how xenobiotics affect human placentation.

Objectives: This study aimed to screen and identify placentation-disrupting chemicals in commonly used organophosphate flame retardants (OPFRs) and, if identified, to investigate potential adverse effects on placentation in relation to adverse pregnancy outcomes and metabolic disorder in offspring in mice.

Methods: We devised a high-throughput immunofluorescence screening assay based on human trophoblast organoids and used it to screen OPFRs that inhibit the proliferation of organoids. One identified chemical was assessed for its effects on placentation by evaluating villous cytotrophoblasts, syncytiotrophoblasts, and extravillous trophoblasts using immunofluorescence and a mitochondrial stress test after 2 d of exposure. A 10-d exposure study was further performed to observe the dynamic effect of the OPFR on the structure of the organoids. RNA-sequencing and western blotting experiments were performed to explore the associated pathways, and a potential binding protein was identified by immunoprecipitation and *in vitro* kinase activity assays. Animal studies were performed to determine whether the findings in organoids could be replicated in mice and to observe adverse pregnancy outcomes.

Results: The proliferation of organoids exposed to three aryl-OPFRs was significantly lower than the proliferation of control organoids. Further analysis demonstrated that one such chemical, 2-ethylhexyl-diphenyl phosphate (EHDPP), disrupted placentation in organoids. Mechanistically, EHDPP interfered with insulin-like growth factor 1 receptor (IGF1R) to inhibit aerobic respiration. Mice exposed to EHDPP at a physiological human concentrations exhibited immature and mature placental disorders, which correlated with fetal growth restriction, implantation failure, stillbirth, and impaired glucose tolerance.

Conclusions: The human trophoblast organoid model showed that the commonly used OPFRs disrupted placentation via IGF1R, indicating that its use may contribute to adverse pregnancy outcomes and metabolic disorders in offspring. https://doi.org/10.1289/EHP10273

Introduction

The incidence rates of adverse pregnancy outcomes, including preeclampsia[1] and fetal growth restriction (FGR),[2] together with adult metabolic diseases such as type 2 diabetes,[3] are steadily increasing. The trends in the incidence of such diseases have developed in a timeframe inconsistent with the much slower pace of changes in the human genome,[4] suggesting that environmental factors have shaped these disease patterns. Reports by the International Federation of Gynecology and Obstetrics,[5] the World Health Organization, the United Nations Environment Program,[6] the American Academy of Pediatrics,[7] and the Endocrine Society[8,9] indicated that early-life chemical exposure can cause serious adverse effects during susceptible periods of human development that endure into later life. Identification of the environmental chemicals that may induce adverse pregnancy outcomes and adult metabolic diseases is essential.

Epidemiological studies have linked environmental chemicals such as bisphenol A, phthalates, perfluoroalkyl acids, and organophosphate flame retardants (OPFRs) to adverse pregnancy outcomes and adult metabolic diseases.[10] Because human population studies were complicated by the diverse genetic backgrounds of the subjects and their concurrent exposure to numerous chemicals, these studies often yielded heterogeneous results and may not provide direct evidences of causal relationships.[11] As a crucial organ in the regulation of fetal development, the placenta is responsible for secretion of hormones that reprogram maternal physiology and for maternal–fetal material exchange. Cumulative evidence suggested that placental disorders can induce adverse pregnancy outcomes and, by the "thrifty phenotype hypothesis," permanently alter human metabolism and increase the risk of lifelong metabolic diseases.[12,13] Placenta develops from trophoblasts to mature placenta during the first trimster of human pregnancy. Placentation is particularly essential because it models the basic pattern of materal–fetal interaction and gradually promotes maternal adaptation to invasive tissue.[14] However, whether and how a xenobiotic affects human placentation remains unknown, owing to limited access to developing human placenta tissues and absence of practical experimental models.

Because adverse effects assessed using cell lines lack relevance for human health, directly modeling complex human disease and tissue biology using high-throughput assays is desirable, as proposed in the ToxCast program of the U.S. Environmental Protection Agency.[15,16] Recently developed human trophoblast organoids displayed near-physiological cellular composition and behavior relative to immature human placenta and allowed dynamic placentation to be observed.[17] Establishing a high-throughput screening model using human trophoblast organoids may be desirable in identifying a chemical that may disrupt human placentation from a wide range of chemicals.

Here, we devised a high-throughput immunofluorescence screening assay based on human trophoblast organoids and used it to screen for OPFRs that could inhibit proliferation. OPFRs as substitutes for conventional flame retardants are commonly used in furniture and electronic productions[18] and have been detected

*These authors contributed equally to this work.

Address correspondence to Jianying Hu, MOE Laboratory for Earth Surface Process, College of Urban and Environmental Sciences, Peking University, Beijing, 100871, China. Email: hujy@urban.pku.edu.cn

Supplemental Material is available online (https://doi.org/10.1289/EHP10273).

All authors declare they have no actual or potential competing financial interests.

Received 8 September 2021; Revised 8 March 2022; Accepted 28 March 2022; Published 3 May 2022.

Note to readers with disabilities: *EHP* strives to ensure that all journal content is accessible to all readers. However, some figures and Supplemental Material published in *EHP* articles may not conform to 508 standards due to the complexity of the information being presented. If you need assistance accessing journal content, please contact ehpsubmissions@niehs.nih.gov. Our staff will work with you to assess and meet your accessibility needs within 3 working days.

in humans worldwide.[19,20] We used short-term and long-term exposure strategies to investigate the effects of one such chemical, 2-ethylhexyl-diphenyl phosphate (EHDPP), on placentation in trophoblast organoids and the associated molecular mechanisms because EHDPP has been widely detected in both the environment[21] and the human body.[22] Finally, the possible occurrence of disorders in immature and mature placentas and adverse pregnancy outcomes were investigated in mice.

Materials and Methods

We performed model validation, high-throughput screening, and short- and long-term exposure studies and explored the associated mechanisms in organoids. Animal studies were also performed. The experiments and their aims are summarized in Figure 1.

Chemicals and Reagents

Forty-six OPFRs were included in the screening list (Table S1). Thirty OPFRs for which standards could be obtained commercially were picked from Toxicity Forecaster (ToxCast) list (https://comptox.epa.gov/dashboard/chemical-lists/FLAMERETARD). Sixteen OPFRs that were recently identified in the environment were also included in the OPFR list, and their relevant context related to where in the environment they were found is described in Table S2. The stock solution for each OPFR standard (10 mM) was prepared in dimethylsulfoxide (DMSO). Triphenyl-d_{15} phosphate (TPhP-d_{15}) purchased from C/D/N Isotopes Inc. was used as the internal standard for EHDPP analysis. Other chemicals used in this paper are detailed in Table S3.

Human Samples

Human villi were collected from five 25- to 40-y-old donors. The age and gestational age of the donors and the karyotypes of the villi are presented in Table S4. All human villi used in this study were attained with written patient-informed consent (PIC) in accordance with the guidelines in the 2000 Declaration of Helsinki. Elective terminations of normal pregnancies at 6–9 wk of gestation were performed at Peking University People's Hospital under ethical approval from the institution (2018PHB060-01). The presence of a fetal sac, limb buds, and fetal heartbeats in the donors was confirmed by ultrasonography prior to the surgical operation. The villi were separated immediately after the operation and stored in Dulbecco's modified Eagle's medium (DMEM)-F12 (11330032; Thermo Fisher Scientific) in 50-mL amicrobic centrifuge tubes (430828; Corning, Inc.) at room temperature. The villi were then transformed to organoids within 3 h of collection. Organoids from Donor 1 (Table S4) were used in all experiments, whereas the other organoids were used only to assess the effects of EHDPP on organoid proliferation.

Organoid Culture

According to the recently reported protocol,[23] trophoblast organoids (Figure S1A–B) were induced from villi in first trimester placental tissue. Briefly, the villus was digested with 0.25% Trypsin-EDTA (25200056; Thermo Fisher Scientific) and DNase I (M0303S; New England Biolabs, Inc.) and then cultured in trophoblast organoid medium (TOM) for 7–10 d (Table S5). The formed organoids were digested for passage using Tryple Express (12604013; Thermo Fisher Scientific). A blood counting chamber (YA0810; Solarbio) was used to count cells in the organoid cell pellets, and the diameter of the organoids was determined using a Leica DMI8 inverted microscope (Leica Microsystems) after digestion and resuspension in TOM. Organoids were maintained at 37°C in a humidified atmosphere of 5% CO_2 and were digested at 37°C for 5 min to form small cell pellets (10–50 μm in diameter). After centrifugation at 600 rpm for 6 min, undiluted digested organoids were resuspended in Matrigel (356231; Corning, Inc.). Twenty microliters of Matrigel were added to each well of a 24-well plate, and the plate was incubated at 37°C for 10 min. Subsequently, 500 μL of TOM was added to culture the organoids.

Screening and Toxicity Evaluation

For time- and cost-efficient toxicity screening, we optimized the digestion and culture protocols. In the optimized protocol, the organoids were digested at 37°C for 3 min and then gently pipetted up and down to yield large cell pellets (50 μm in diameter for >50% of the pellets; "optimized digestion"; Figure S1C). To maintain rapid proliferation, the concentrations of CHIR99021, Y27632, and prostaglandin E_2 (PG E_2) in TOM were increased to 5, 10, and 10 μM, respectively (Table S2, "Optimized TOM"), as these chemicals have been reported to increase proliferation.[24–26] Undiluted cell pellets were replated onto 96-well plates with 10 μL Matrigel at a density of 3,000 pellets per well. After a 2-d culture, trophoblast organoids were treated with each chemical from the list of OPFRs (Table S1) at 10,000 nM. The same DMSO concentration (0.1%) used in the exposure groups was used in the control group ($n = 3$). Sytox Green (R37168; Thermo Fisher Scientific) was used to evaluate cell survival.[27] In the screening assay, 2-d OPFRs exposure was performed considering both fast screening and toxicity observation. After the organoids were exposed to OPFRs, Sytox Green (dilution: 1:50) was added, followed by incubation at 37°C for 30 min. Thereafter, fluorescence was measured using an ImageXpress Micro Automated High-Content Analysis System (Molecular Devices).

This study used Ki67 to evaluate proliferation of organoids. After exposure to OPFRs for 2 d, the organoids were fixed with 4% paraformaldehyde (C2055; Bioss) for 30 min at room temperature, permeabilized by 0.25% Triton X-100 (CR00576; EBT Systems) for 30 min at room temperature, blocked in 3% bovine serum albumin (BSA) (PM5130; Coolaber) in phosphate-buffered saline (PBS) for 60 min at 37°C, and stained with an anti-Ki67 antibody (9449S; dilution: 1:100; Cell Signaling Technology) for 60 min at 37°C and with secondary antibodies (antimouse IgG heavy and light chains, 8890S, dilution: 1:100, Cell Signaling Technology) for 60 min at 37°C. After Ki67 incubation and secondary antibody incubation, the organoids were washed three times with PBS. These steps were followed by automatic imaging and analysis using an ImageXpress Micro High-Content Analysis System (Molecular Devices) to obtain the fluorescence intensity.

The EHDPP concentration of 10,000 nM has been reported to be the lowest observed effect concentration to disrupt hormone biosynthesis in human choriocarcinoma cell line.[28] Thus, exposure concentration was set at 100–10,000 nM for obtaining dose-dependent placental-disrupting effects. Organoids were exposed to 100, 1,000, or 10,000 nM EHDPP on the third day after digestion and were then cultured for an additional 2 d, in which the exposure timing was determined similar with screening assay. The same DMSO concentration (0.1%) was used in the exposure groups and the control group ($n = 3$).

To observe the dynamic effects of EHDPP on placentation, organoids were exposed to 100, 1,000, or 10,000 nM EHDPP on the third day after digestion and were then cultured for an additional 10 d following the protocol described in the "Organoid Culture" section. The timing of long-term exposure was set as 10 d, which is the longest timing of culture reported previously.[23] The same DMSO concentration (0.1%) was used in the exposure groups and the control group ($n = 3$).

Processes	Indicators and methods	Aims
Model validation 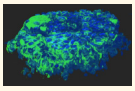	Morphologic observation KRT7, GATA3 (Immunofluorescence) hCG, E2 (Elisa)	Validating the previous and optimized trophoblast organoid models
High-throughput screening 46 OPFRs (10,000 nM) 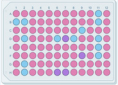 (Created with BioRender.com)	Ki67 (Immunofluorescence)	Organoids proliferation
	Sytox Green	Cell survival
Short-term exposure (100, 1,000, 10,000 nM EHDPP)	Ki67, TP63, CD71, HLA-G(Immunofluorescence)	Organoids proliferation, VCT, SCT and EVT
	Aerobic respiratory (Mitochondrial stress assay)	Aerobic respiratory levels
	PD (Western blotting)	TCA cycle
	Ki67 of organoids from 5 donors (1000 nM EHDPP, Immunofluorescence)	Individual differences
Long-term exposure (100, 1,000, 10,000 nM EHDPP)	Ki67, TP63, CD71, HLA-G (Immunofluorescence)	Organoids proliferation, VCT, SCT and EVT
	hCG, E2	Secretion functions of organoids
Mechanism (100, 1,000, 10,000 nM EHDPP without special instructions)	RNA-seq	Mechanism study
	p-IGF1R, IGF1R, p-Akt, Akt (Western blotting)	IGF1R-Akt signaling activity
	IGF1,IGF2 (RT-qPCR)	IGF1 and IGF2 expression
	Directly binding effect (1,000 and 10,000 nM EHDPP, Immunoprecipitation) Inhibition of tyrosine kinases activity *in vitro* (1, 10, 100, 1,000, 10,000 nM EHDPP and 0.001, 0.01, 0.1, 1, 10, 100 nM OSI-906)	EHDPP directly binds to IGF1R and inhibit its function *in vitro*
	Ki67, TP63, CD71, HLA-G (50 nM OSI-906, Immunofluorescence)	Organoids proliferation, VCT, SCT and EVT in positive IGF1R inhibitor exposure
Animal study (0.4, 2, 10 mg/kg day EHDPP without special instructions)	Cdx2, Ki67 (10 mg/kg day EHDPP, Immunofluorescence)	Abnormal placentation in immature placenta
	TPBPA, TFAP2C, HAND1 (10 mg/kg day EHDPP, Immunofluorescence)	Disorder in mature placenta
	p-IGF1R, IGF1R, PD, Cyto C (Western blotting) p-IGF1R (10 mg/kg day EHDPP, Immunofluorescence) RNAseq	EHDPP inhibit IGF1R and aerobic respiratory in placenta
(Created with BioRender.com)	Implanted embryos and survival embryos counting FGR analysis OGTT	Outcomes

Figure 1. Summary of methods. Note: Akt, protein kinase B; CD71, transferrin receptor; Cyto C, cytochrome C; E_2, estradiol; EHDPP, 2-ethylhexyl-diphenyl phosphate; EVT, extravillous trophoblast cell; FGR, fetal growth restriction; GATA3, GATA-binding protein 3; HAND1, crest derivatives-expressed protein 1; hCG, human chorionic gonadotropin; HLA-G, human leukocyte antigen protein-G; IGF, insulin-like growth factor; IGF1R, insulin-like growth factor 1 receptor; KRT7, keratin 7; OGTT, oral glucose tolerance test; OPFRs, organophosphate flame retardants; OSI-906, linsitinib; p-Akt, phosphorylated Akt; PD, pyruvate dehydrogenase complex; p-IGF1R, phosphorylated IGF1R; RNA-seq, RNA sequencing; SCT, syncytiotrophoblast; TCA, tricarboxylic acid cycle; TFAP2C, transcription factor AP-2γ; TP63, tumor protein 63; TPBPA, trophoblast-specific protein α; VCT, villous cytotrophoblast.

Quantitative Real-Time Polymerase Chain Reaction (qPCR)

Trophoblast organoids or animal tissue samples were collected using 500 μL TransZol Up (ET111-01, Transgen). For RNA extraction, 100 μL of chloroform (M1024442500; Merck) was added to each sample, and the samples were shaken vigorously and centrifuged at 12,000 rpm for 10 min at 20°C. The resulting top layer was aspirated, and an equal volume of isopropyl alcohol (1.01,040.4008; Merck) was added. The samples were shaken gently and centrifuged at 12,000 rpm for 10 min at 20°C. After

removing the supernatant, 700 μL of 75% ethanol (E801077; Macklin) was added, and the samples were shaken gently and centrifuged at 12,000 rpm for 5 min at 20°C. The supernatant was removed, and the RNA pellet was dissolved in 30 μL of diethyl pyrocarbonate-treated H_2O (W274329; Aladdin). The RNA samples were then quantified using a Nanovue Plus spectrophotometer (GE Healthcare Life Science). We used Oligo dT (3805; Takara), Moloney Murine Leukemia Virus Reverse Transcriptase (639574; Takara), Recombinant RNase Inhibitor (2313Q; Takara), dNTP (4019; Takara), and Random Primers (3802; Takara) for reverse transcription on a S1000 Thermal Cycler (Bio-Rad) with the following program: 40°C for 60 min, 70°C for 15 min, and held at 4°C. SYBR Green (QPK-201; Toyobo) was used for real-time fluorescence detection on a StepOnePlus sequence detection system (Applied Biosystems) with the following program: 95°C for 1 min and 40 cycles of 95°C for 15 s and 60°C for 45 s. Relative gene expression was evaluated by the $2^{-\Delta\Delta Ct}$ method, as suggested by Applied Biosystems. The primers were synthesized by Thermo Fisher Scientific, and the primer sequences are listed in Table S6.

Immunofluorescence of Organoids

After EHDPP exposure, trophoblast organoids were fixed with 4% paraformaldehyde for 30 min, permeabilized by 0.25% Triton X-100 for 30 min, blocked in 3% BSA in PBS for 60 min at 37°C, and stained with primary antibodies for 60 min at 37°C and secondary antibodies for 60 min at 37°C. After primary and secondary antibody incubation, the organoids were washed three times in PBS. Information regarding the antibodies and 4′,6-diamidino-2-phenylindole (DAPI) is provided in Table S7. Samples were visualized under a Dragonfly High Speed Spinning Disk Confocal Microscope (Oxford Instruments Andor) and were quantified using Fiji software.[29]

Enzyme-Linked Immunosorbent Assay (ELISA)

Estradiol (E_2) is not independently synthesized in the placenta because placenta does not biosynthesize its precursor; therefore, it is mainly transported after maternal and fetal synthesis.[30] Thus, the organoid culture medium was supplemented with testosterone (40 μM) after a 1-d culture to determine the E_2 secretion capacity of the organoids. To assess hCG-β and E_2 secretion, the collected medium was centrifuged at 12,000 rpm for 10 min to remove debris and then stored at −80°C. An hCG-β ELISA (48T-QS40792; Qisong Bio.) and E_2 ELISA (APH102; Tiosbio) were performed using 50 μL supernatant and 50 μL sample dilution buffer. The concentrations of hCG-β and E_2 were measured by absorbance at 450 nm using a microplate reader (SpectraMax i3X; Molecular Devices) following the manufacturer's protocol.

Mitochondrial Stress Assay

Trophoblast organoids were cultured in 24-well tissue culture plates (100882; Agilent) at a density of 5,000 cell pellets per well and exposed to EHDPP for 48 h. The sensor cartridge was then hydrated overnight in Seahorse XF Calibrant (100850; Agilent) at 37°C in a non-CO_2 incubator. Before analysis of the oxygen consumption rate (OCR), cells were reconstituted for 60 min in an extracellular flux (XF) base medium containing 100 mM pyruvate, 200 mM glutamine, and 2.5 M glucose at pH 7.4. Chemical reagents were used at the following final concentrations: 1 μM oligomycin, 2 μM carbonyl cyanide-4 (trifluoromethoxy) phenylhydrazone (FCCP), 0.5 μM antimycin A, and 0.5 μM rotenone.

RNA Sequencing

The mRNA was extracted from trophoblast organoids or placentas of E19.5 mice using TransZol Up (ET111-01, Transgen) ($n = 3$). Briefly, the placentas were homogenized in tubes containing 500 μL of TransZol Up using an electric homogenizer. RNA was extracted using chloroform (M1024442500; Merck) and purified using isopropyl alcohol (1.01040.4008; Merck) and 75% ethanol (E801077; Macklin), as detailed in the "Quantitative Real-Time Polymerase Chain Reaction (qPCR)" section. The RNA quality and concentration were determined using a Nanodrop ND-1000 spectrophotometer (Nanodrop Technologies). RNA samples with an RNA integrity number >7 were considered to be qualified for RNA sequencing (RNA-seq). RNA-seq was performed at Beijing Genomics Institute. RNA samples were enriched for poly A species, and the sequencing libraries were constructed and then sequenced on a BGISEQ-500 platform (BGI). The average fragment size and overall quality were determined using an Agilent 2,100 Bioanalyzer. Each library was sequenced to an approximate depth of 40 million reads. Sequencing data were filtered using SOAPnuke (version 1.5.2; BGI-FlexLab).[31] Sequencing reads were mapped against GRCh38.p12 (human trophoblast organoids) or GRCm38/mm10 (mouse placenta) reference genomes using HISAT2 (version 2.0.4; Lady Hill Department of Bioinformatics)[32] and Bowtie2 (version 2.2.5; Langmead lab at Johns Hopkins University).[33] The gene expression levels in each sample were calculated using RNA-Seq by Expectation-Maximization (version 1.2.8), and differentially expressed genes were identified using DEGseq2 (version 1.34.0; Mike Love). Only protein-coding genes, processed pseudogenes, and lncRNAs were included in the analysis.

Cell Culture of 293T

The 293T cell line was purchased from American Type Culture Collection. 293T cells were cultured in DMEM (C11995500 BT; Thermo Fisher Scientific) supplemented with 10% FBS (10099141C; Gibco). 293T cells were maintained in a humidified atmosphere of 5% CO_2 at 37°C.

Western Blotting Analysis

Trophoblast organoids, cells, and animal tissue samples were collected in cell lysis buffer (9803S; Cell Signaling Technology, Inc.) with PhosStop (4906837001; Coolaber), and the protein concentrations were measured by BCA protein assay (P0012S; Beyotime). The samples ($n = 3$) were centrifuged at 12,000 rpm for 10 min at 4°C, and the resulting supernatants were retained for subsequent experiments. After adding 5× loading buffer to each sample, the mixtures were then heated to 100°C for 5 min. Samples were loaded at 30 μL per lane of a polyacrylamide gel. The final protein concentration was 3 μg/μL, and 90 μg of total protein was run per lane. The proteins were transferred to a nitrocellulose (NC) membrane (MH0322; Macklin) and subsequently blocked with 3% BSA in TBST (50 mM Tris–HCl at pH 8.0, 150 mM NaCl, 0.1% Tween-20) for 60 min at room temperature. The membrane was then incubated with the primary antibody at 4°C for 24 h and then with the secondary antibody at room temperature for 1 h. After primary and secondary antibody incubation, the organoids were washed three times with TBST (10 min each time). To normalize phosphorylated protein levels, the blots that were probed for phosphorylated proteins were stripped to allow the determination of total protein content. The membranes were washed twice with TBST (10 min each time) and then shaken in stripping buffer (25 mM glycine-HCl, pH 2.0; PMC1710125; Perfemiker) and 1% SDS (CS9701-100g; Coolaber) at 100 rpm for 25 min at room temperature. The

membranes were washed another two times after stripping and were then blocked, incubated with primary and secondary antibodies, and washed following the protocols described above. Antibody information is provided in Table S7.

Immunoprecipitation

To evaluate the binding activity of EHDPP to IGF1R, immunoprecipitation was performed using 293T cells. 293T cells were cultured in a 10-cm petri dish at a density of $20{,}000/cm^2$ overnight, followed by transfection with pcDNA3.1 IGF1R-BirA (R118G)-hemagglutinin (HA) and pcDNA3.1 GFP-HA plasmids using Lipofectamine 2000 Transfection Reagent (11668027, Thermo Fisher Scientific; $n=3$). The plasmid pcDNA3.1 IGF1R-BirA(R118G)-HA was obtained from Addgene, Inc. The plasmid pcDNA3.1 GFP-HA was constructed by Beijing Genomics Institute based on pcDNA3.1 IGF1R-BirA(R118G)-HA. The sequence of this plasmid is provided in the Supplemental Material ("Sequence of HA-GFP" section). The transfected cells were exposed to EHDPP at 1,000 or 10,000 nM for 48 h, and the total protein was then collected by cell lysis buffer (9803S; Cell Signaling Technology, Inc.). The collected samples were centrifuged at 12,000 rpm for 10 min at 4°C, and the supernatant was collected for subsequent experiments. A HA-Tag Magnetic immunoprecipitation/co-immunoprecipitation (IP/co-IP) kit (88838; Thermo Fisher Scientific) was used in the immunoprecipitation experiment. HA-IGF1R and HA-GFP proteins were captured by immunoprecipitation using anti-HA beads, respectively. The target protein was collected in elution buffer and diluted to 1 mL by PBS. After adding $TPhP\text{-}d_{15}$ as an internal standard, ethyl acetate (3 mL) was added to extract the EHDPP bound with the protein. The mixtures were then shaken for 20 min on an orbital shaker, followed by 4,000 rpm centrifugation for 12 min. Extraction from the residues was repeated twice. The extracted samples were dissolved with 1 mL of hexane (Hex). Samples were preconditioned with 6 mL of dichloromethane (DCM), 6 mL of Hex, and 6 mL of Hex/DCM (80:20, v/v). After that, samples were loaded onto Bond Elut NH_2 (6 mL, 1 g) cartridges. After washing with Hex (3 mL) and Hex/DCM (1.5 mL, 80:20, v/v), DCM (3 mL) was used to elute the analytes from the NH_2 cartridges. The extracts were evaporated to dryness under high-purity nitrogen. After that, the extracts were redissolved in 100 μL of methanol (MeOH) for liquid chromatography–tandem mass spectrometry (LC-MS/MS) analysis. The LC apparatus was an UltiMate 3000 UHPLC system (Thermo Fisher Scientific). The column (C8) was maintained at 40°C with a flow rate of 0.3 mL/min, and the injection volume was 5 μL. Methanol (A) and ultrapure water containing 10 mM ammonium acetate (B) were used as the mobile phases. The mobile phase gradient was increased from 10% to 40% solvent A linearly within 1 min. Solvent A was then increased to 100% in the next 9 min and maintained at 100% for 3.5 min. Finally, the gradient was returned to the initial condition of 10% solvent A for a 6 min re-equilibration before the next injection. The total run time was 18.5 min. Mass spectrometry was performed using a TSQ Quantum Ultra mass spectrometer (Thermo Fisher Scientific) equipped with a Z-Spray ionization source operated in the positive ion mode. The ion transfer tube temperature, vaporizer temperature, sheath gas, aux gas, and spray voltage were 320°C, 200°C, 40 Arb, 12 Arb, and 3,200 V, respectively. The recovery of EHDPP was $87.6 \pm 13\%$. The limit of quantitation (LOQ) was 0.022 ng/mL, and the final concentrations reported in this study were blank subtracted (0.007 ± 0.0015 ng/mL).

Concentration Determination of EHDPP in Organoids

Organoids were exposed to 1,000 nM EHDPP on the third day after digestion and were then cultured for an additional 2 d, following the protocol described in the "Screening and Toxicity Evaluation" section; the blank samples were prepared by DMSO-treated organoids, following the same protocol ($n=3$). After that, the organoids were digested by Tryple Express, followed by 1,000 rpm centrifugation for 5 min at 4°C. After removing the supernatant, organoids were freeze-dried and then dissolved and detected, following the protocol described in the "Immunoprecipitation" section. The LOQ was 103.0 ng/g dry weight (dw), and the final concentrations reported in this study were blank subtracted (73.4 ± 3.0 ng/g dw).

In Vitro Kinase Activity Test

Because IGF1R is a tyrosine kinase receptor, this study performed *in vitro* kinase activity test to demonstrate that EHDPP can bind to IGF1R and inhibit its kinase activity *in vitro*. This study used Z′-LYTE kinase assay kit-Tyr 1 peptide (PV3190; Thermo Fisher Scientific) and IGF1R recombinant human protein (PV3592; Thermo Fisher Scientific; 150 ng/mL in the test). This study detected the kinase activity of 0.1, 1, 10, 100, 1,000, and 10,000 nM EHDPP and 0.001, 0.01, 0.1, 1, 10, and 100 nM OSI-906 (positive antagonist of IGF1R), and DMSO was used as the control ($n=3$). The mix of 2.5 μL compound, 5 μL kinase/peptide, and 2.5 μL adenosine triphosphate (ATP) solution was incubated for 60 min at room temperature. The mix of 2.5 μL DMSO, 5 μL kinase/peptide, and 2.5 μL kinase buffer was used as a 100% inhibition control group; the mix of 2.5 μL DMSO, 5 μL kinase/peptide, and 2.5 μL ATP solution was used as a 0% inhibition control group; and the mix of 2.5 μL DMSO, 5 μL phosphopeptide solution, and 2.5 μL kinase buffer were used as a 100% phosphorylation control group. After that, 5 μL development solution was added for 60 min at room temperature, and then 5 μL stop reagent was added. The mixes were detected at Ex400, Em445, and Em520, using a microplate reader (SpectraMax i3X; Molecular Devices). The protocol was detailed in https://www.thermofisher.cn/order/catalog/product/PV3190?SID=srch-srp-PV3190.

Animal Experiments

Animal studies were performed in accordance with the University Guidelines for Animal Experiments and were approved by the Institutional Animal Care and Use Committee of Peking University (approved No. Urban-HuJY-1). Female 8-wk-old CD-1 mice and male 10-wk-old CD-1 mice from Charles River Laboratories were used in this study. All female mice used in this experiment were acclimated in the housing units for 10 d prior to the experiment and were assigned to each group randomly ($n=10$ per group). Two female animals were housed to a cage, and the mice were acclimatized to the controlled environment (artificial lighting: 12-h/12-h light/dark photoperiod; temperature: $22° \pm 2°C$; relative humidity: 40%–60%). After the acclimatization period, EHDPP was dissolved in edible oil (peanut oil; Arawana) and administered to the female mice at 0, 0.4, 2, or 10 mg/kg/d by gavage. Edible oil was used as a control. Considering that the substances in pregnant women come not only from exposure during pregnancy but also from the exposure before pregnancy, this study exposed female mice 2 wk before pregnancy. After 2 wk of exposure, the female mice cohabited with the untreated male mice at a ratio of 2:1, and vaginal plug formation was checked the following morning as a marker of successful mating. After fertilization, the female mice were continuously exposed to EHDPP until E19.5, and then the mice were anesthetized by 100 mg/kg sodium pentobarbital via intramuscular injection and euthanized via cervical dislocation. The embryos were weighed and dissected, and the dead fetuses and resorption rates were counted. Every E19.5 placenta in this study was from a different dam, which was picked randomly. E19.5 placentas were collected for EHDPP analysis ($n=3$), immunofluorescence ($n=5$), western blotting ($n=3$), and RNA-seq ($n=3$).

The EHDPP concentration was analyzed using LC-MS/MS. Placental samples were freeze-dried and ground into fine powder and spiked with a 1 ng TPHP-d_{15} internal standard. The details of the extraction and LC-MS/MS methods are described in the "Immunoprecipitation" section. The recovery of TPHP-d_{15} was 58.6% ± 4%, and the recovery of EHDPP was 60.4% ± 13%. The LOQ was 0.169 ng/g dw. The final concentrations reported in this study are blank subtracted (0.033 ± 0.014 ng/g dw). E19.5 fetuses were born by cesarean section, and their body weight (BW) was measured immediately. Resorbed, stillborn, and surviving fetuses were counted, and the implantation number was calculated by adding the number of live births, resorbed fetuses, and stillborn fetuses. In humans, FGR is defined as a birthweight lower than the 10th percentile.[34] By using the definition of human FGR and the weight distribution of control mice, the fetal mice with the weight lower than 1.371 g were identified as FGR mice, and then we calculated the corresponding incidence of FGR for each treatment group. Oral glucose tolerance tests (OGTT) were performed in 8-wk-old offspring of dams in the control and in the 0.4, 2, 10 mg/kg EHDPP exposure groups. Every 10 offspring (5 males and 5 females) of dams were used in this study. These offspring were not exposed to EHDPP after birth. One male and one female offspring without observable defect from a dam were picked for glucose tolerance tests, and the weight of the early groups including 10 offspring have no significant difference. Offspring were fasted for 16 h before the test and were then administered 2 g/kg glucose (D5796; Sigma) by gavage. Orbital blood samples (100 μL) were collected from each offspring at 0, 15, 30, 60, and 90 min after gavage. Serum was separated by centrifuging blood samples at 4,000 rpm and 4°C for 5 min, and blood glucose concentration was determined using a glucose testing kit (PS0382; Psaitong).

Immunofluorescence of E7.5 Embryos

After 2 wk of EHDPP exposure, the female mice were cohabited with the normal male mice at a ratio of 2:1, and vaginal plug formation was checked the following morning as a marker of successful mating. After fertilization, the female mice were continuously exposed to EHDPP until E7.5, and then the mice were anesthetized by sodium pentobarbital via intramuscular injection and euthanized via cervical dislocation ($n = 5$). Every E7.5 embryos in this study were from different dams, which were picked randomly. The embryos were collected for whole-mount immunofluorescence by a previously reported method.[35] E7.5 embryos were fixed with 4% paraformaldehyde and 0.1% Triton X-100 for 2 h at room temperature; permeabilized by 1% Triton X-100 for 8 h at room temperature; blocked in 10% BSA, 5% donkey serum (P05B58S; GPL), and 0.1% Triton X-100 for 2 h at room temperature; and then incubated with a primary antibody overnight at 4°C and with secondary antibodies for 2 h at 37°C. Antibody and DAPI information is provided in Table S7. Samples were visualized under a Dragonfly High Speed Spinning Disk Confocal Microscope and quantified using Fiji software.[29]

Immunofluorescence of E19.5 Placentas

E19.5 placentas were fixed with 4% paraformaldehyde for 1 d ($n = 5$). Every E19.5 placenta in this study was from a different dam, which was picked randomly. After paraffin embedding and dewaxing, the placentas were treated with 3% H_2O_2 (01585853; Adamas) for 15 min and fixed in EDTA (pH = 8) for 3 min. The placentas were blocked in 3% BSA for 30 min at room temperature, followed by incubation with a primary antibody overnight at 4°C and secondary antibodies for 60 min at 37°C. Antibody information is provided in Table S7. Samples were visualized under a fluorescence microscope (BX51; Olympus) and quantified using Fiji software.[29]

Statistical Analyses

GraphPad Prism (version 9.0.0; GraphPad Software) was used to perform all statistical analyses. The unpaired two-tailed Student's *t*-test with or without Welch's correction and the chi-square test was used for multiple comparisons; $^{*}p < 0.05$ and $^{**}p < 0.01$ were considered to be statistically significant. All exposure experiments of organoids were performed in triplicates. The screening, ELISA test, mitochondrial stress assay, EHDPP concentration detection, *in vitro* kinase activity test, and glucose concentration test of OGTT had three technical replicates. Western blotting and qPCR had two technical replicates. RNA-seq had no technical replicate. Each organoid treatment experiment was performed in triplicate. Each immunofluorescence of organoids had five randomly selected microscopic fields. Experiments that involved counting birth weight of fetuses, implanted embryonic numbers, and surviving embryonic numbers were performed twice with $n = 5$ and $n = 5$, and E19.5 placentas were selected randomly from each second experiment, respectively. The exposure experiment of immunofluorescence of E7.5 was performed once with $n = 5$.

Data Availability

The data that support the findings of this study are available from the corresponding author on request. RNA-Seq data is available in Excel Table S1 and Excel Table S2.

Results

Trophoblast Organoid-Based Screening of OPFRs at 10,000 nM

This study used trophoblast organoids to investigate the toxicity of chemicals in human placentation. We followed an existing protocol[23] to produce the trophoblast organoids (Figure S1A, S1B). This study digested organoids to yield cell pellets (50 μm in diameter for >50% of pellets; Figure S1C). Over half the pellet cells reached a diameter of approximately 100 and 200 μm after 2- and 4-d cultures, respectively (Figure 2A), whereas the proliferation of organoids in optimized digestion was 0.85- ± 0.06-fold relative to the previous digestion after 2-d culture (Figure S1D). After increasing the concentrations of CHIR99021, Y27632, and PG E_2 in TOM (Table S5), the proliferation of organoids in optimized TOM was 1.17 ± 0.04-fold relative to the previous TOM after 2-d culture (Figure S1E). The trophoblast identity of the newly cultured organoids was verified by the expression of markers, including keratin 7 (KRT7) and GATA binding protein 3 (GATA3) (Figure 2B) and by secretion of E_2 and human chorionic gonadotropin (hCG). The concentrations of hCG and E_2 in the organoids were 10,227 ± 473 mIU/mL and 25,623.5 ± 2110.4 pg/mL, respectively, during 24 h of secretion. This study detected cell proliferation and survival by using Ki67 and Sytox Green, respectively, and then assessed the effects of exposure to 46 existing and emerging OPFRs. Any chemicals that caused more than a 20% reduction in Ki67 expression and did not significantly affect cell survival were picked as positive hits (Figure 2C,D). Under these criteria, three aryl-OPFRs—EHDPP, tri-o-cresyl phosphate (o-TCrP), and bis (4-tert-butylphenyl) phosphate (B4tBPPP)—were identified as positive hits (Figure 2E). The numeric data from the screening experiments are listed in Table S8.

Short- and Long-Term Toxicity of EHDPP in Organoids

In this study, trophoblast organoids were exposed to EHDPP at 100, 1,000, and 10,000 nM. Cells exposed to EHDPP did not exhibit significantly higher rates of cell death at these concentrations after 2 or

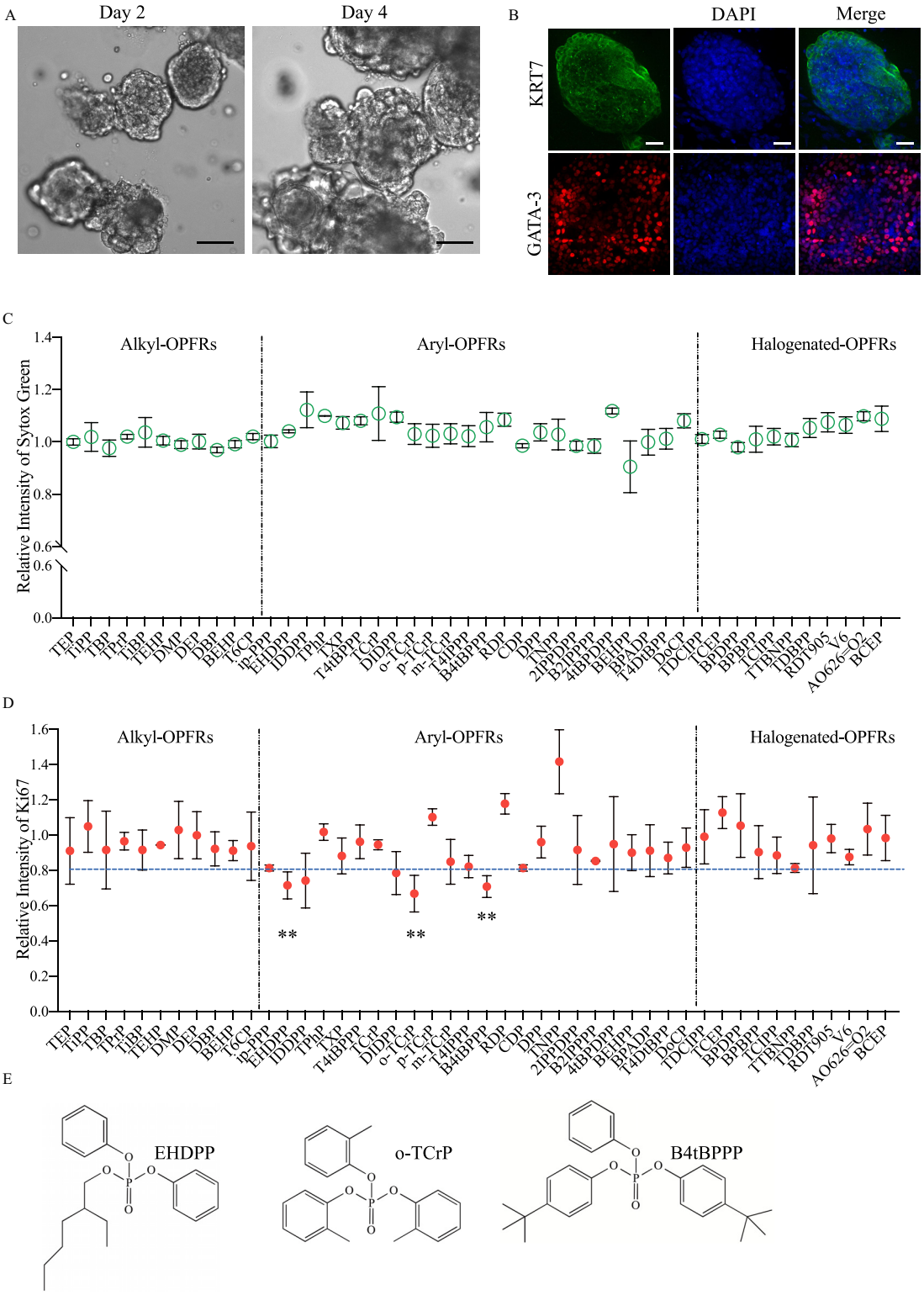

Figure 2. Trophoblast organoid-based screening of OPFRs at 10,000 nM. (A) 2- and 4-d culture of trophoblast organoids in screening protocol and scale bars, 100 μm; (B) Immunofluorescence of villus markers KRT7 (green), GATA3 (red), and DAPI (blue) in trophoblast organoids and scale bars, 30 μm; (C) Relative fluorescence intensity (means ± SDs) of Sytox Green (green) in trophoblast organoids exposed to OPFRs (10,000 nM) (D) Relative fluorescence intensity (means ± SDs) of Ki67 (red) in trophoblast organoids exposed to OPFRs (10,000 nM); (E) Structure of identified chemicals, EHDPP, o-TCrP, and B4tBPPP. Data in (C) and (D) are expressed relative to the levels in DMSO-treated organoids, which were set to 1. $n = 3$. All organoids in (C) and (D) were from a single donor. Data were analyzed using an unpaired two-tailed Student's *t*-test. Indicated values are significantly different from the control value. Numeric data in (C) and (D) were listed in Table S8. Note: B4tBPPP, bis (4-tertbutylphenyl) phosphate; DAPI, 4′,6-diamidino-2-phenylindole; DMSO, dimethylsulfoxide; EHDPP, 2-ethylhexyl-diphenyl phosphate; GATA3, GATA-binding protein 3; KRT7, keratin 7; OPFRs, organophosphate flame retardants; o-TCrP, tri-o-cresyl phosphate; SD, standard deviation. $^{**}p < 0.01$.

10 d of exposure (Figure S2A,B). After a 2-d EHDPP exposure, Ki67 expression levels in the 100, 1,000, and 10,000 nM exposure groups were 0.89 ± 0.10, 0.79 ± 0.10 ($p < 0.05$), and 0.48 ± 0.13 ($p < 0.01$) times as high, respectively, as the Ki67 expression levels in the control group (Figure 3A,B). This study tested mitochondrial stress and found that the basic metabolism values in the 100, 1,000, and 10,000 nM exposure groups were $2{,}042.5 \pm 560.4$, $1{,}344.5 \pm 380.9$ ($p < 0.05$), and $1{,}269.1 \pm 252.0$ pmol/min ($p < 0.05$), respectively, which were lower than those in the control group ($3{,}018.1 \pm 740.3$ pmol/min; Figure 3C,D). The respiratory capacity in the 100, 1,000, and 10,000 nM exposure groups was $2{,}383.6 \pm 790.2$, $1{,}643.9 \pm 655.9$ ($p < 0.05$), and $1{,}528.9 \pm 383.4$ pmol/min ($p < 0.05$), respectively, which was lower than those of the control group ($3{,}012.2 \pm 477.8$ pmol/min; Figure 3C,E). Pyruvate dehydrogenase complex (PD) levels in the 100, 1,000, and 10,000 nM exposure groups were 0.84 ± 0.17, 0.69 ± 0.19 ($p < 0.05$), and 0.65 ± 0.20 ($p < 0.05$) times as high, respectively, as those in the control group (Figure S2C,D). Different cell layers of organoids have been further detected, including villous cytotrophoblasts (VCTs), syncytiotrophoblasts (SCTs), and extravillous trophoblast cells (EVTs). TP63 (a specific marker of VCTs) expression levels in the 100, 1,000, and 10,000 nM exposure groups were 0.88 ± 0.13, 0.65 ± 0.12 ($p < 0.05$), and 0.58 ± 0.18 ($p < 0.05$) times as high, respectively, as those in the control group (Figure 3F,G). Additionally, CD71 (a marker of SCTs) expression levels were determined, but they showed no significant difference between the control and EHDPP exposure groups ($p > 0.05$; Figure S2E, F). In addition, human leukocyte antigen (HLA)-G (a marker of EVTs) was not detected (Figure S2G).

After a 10-d EHDPP exposure, Ki67 expression levels in the 100, 1,000, and 10,000 nM exposure groups were 0.95 ± 0.01, 0.80 ± 0.11 ($p < 0.05$), and 0.67 ± 0.12 ($p < 0.05$) times as high, respectively, as those in the control group (Figure 3H,I). TP63 expression levels in the 100, 1,000, and 10,000 nM exposure groups were 0.93 ± 0.23, 0.71 ± 0.16 ($p < 0.05$), and 0.66 ± 0.12 ($p < 0.05$) times as high, respectively, as those in the control group (Figure 3J,K). CD71 expression levels after 10 d of treatment with 100, 1,000, and 10,000 nM EHDPP were 0.67 ± 0.04 ($p < 0.05$), 0.55 ± 0.16 ($p < 0.05$), and 0.51 ± 0.11 ($p < 0.05$) times as high, respectively, as those in the control group (Figure 3H,L). In long-term cultures, HLA-G was detected (Figure 3N), and HLA-G expression levels in the 100, 1,000, and 10,000 nM exposure groups were 0.89 ± 0.21, 0.71 ± 0.16 ($p < 0.05$), and 0.65 ± 0.12 ($p < 0.01$) times as high, respectively, as those in the control group (Figure 3M,N). The concentrations of hCG in the 1,000 and 10,000 nM exposure groups were 0.83 ± 0.02 ($p < 0.01$) and 0.78 ± 0.01 ($p < 0.05$) times as high, respectively, as those in the control group, but no difference was observed between the 100 nM EHDPP exposure and the control group ($p > 0.05$; Figure 3O). The concentrations of E_2 in the 100, 1,000, and 10,000 nM exposure groups were 0.94 ± 0.11, 0.79 ± 0.08 ($p < 0.01$), and 0.72 ± 0.12 ($p < 0.01$) times as high, respectively, as those in the control group (Figure 3P).

In organoids exposed to 1,000 nM EHDPP for 2 d, Ki67 expression levels in the organoids derived from the five donors (Donors #1, #2, #3, #4, and #5) were significantly lower than those in the corresponding control group ($p < 0.05$; 0.77 ± 0.03, 0.75 ± 0.03, 0.73 ± 0.04, 0.83 ± 0.06, and 0.81 ± 0.04 times as high, respectively, as those in the control group; Figure 3Q).

The average concentration of EHDPP in organoids exposed to 1,000 nM EHDPP for 2 d was 610.9 ± 376.4 ng/g dw.

Mechanism of Placentation Disruption

RNA-seq was used to compare global transcript expression profiles between DMSO- and EHDPP-treated trophoblast organoids. The phosphatidylinositol 3 kinase-protein kinase B (P13K-Akt) signaling pathway was found to be significantly enriched, with a lower Q value of 0.0027 and a greater number of enriched genes than other pathways, based on a Kyoto Encyclopedia of Genes and Genomes (KEGG) analysis ($p < 0.01$) (Figure 4A). We found that the relative phosphorylation levels of Akt Ser_{473} in the 100, 1,000 and 10,000 nM exposure groups were 0.71 ± 0.13 ($p < 0.05$), 0.54 ± 0.29, and 0.65 ± 0.03 ($p < 0.01$) times as high, respectively, as those of the control group (Figure 4B,C). We evaluated the levels of phosphorylated insulin-like growth factor 1 receptor (p-IGF1R) in organoids exposed to EHDPP for 2 d. The relative levels of p-IGF1R in the 100, 1,000, and 10,000 nM exposure groups were 0.67 ± 0.16 ($p < 0.05$), 0.56 ± 0.13 ($p < 0.01$), and 0.47 ± 0.25 ($p < 0.05$) times as high, respectively, as those in the control group (Figure 4B, D). Because no significant decrease in expression of IGFs was observed in any of the EHDPP exposure groups when compared with the control (Figure S3A,B), this study detected the binding activity of EHDPP to IGF1R. The amount of EHDPP captured by HA-IGF1R in the 1,000 and 10,000 nM exposure groups was 2.79 ± 0.90 ($p < 0.01$) and 3.12 ± 1.78 ($p < 0.01$) times as high, respectively, as those captured by HA-GFP (Figures S3C,4E). A Z′-LYTE kinase assay was further performed and verified that EHDPP significantly inhibited IGF1R activity with an IC_{50} value of 249 nM [95% confidence interval (CI): 110 nM, 367 nM] (Figure 4F).

After a 2-d exposure to OSI-906, Ki67 and TP63 expression levels in the OSI-906 group were 0.34 ± 0.16 and 0.39 ± 0.14 times as high, respectively, as those in the control group ($p < 0.01$) but without a significant difference in the expression of SCT (Figure 4G,H; Figure S3D–G). After a 10-d exposure to OSI-906, Ki67, TP63, CD71, and HLA-G expression levels were 0.22 ± 0.11, 0.57 ± 0.15, 0.47 ± 0.13, and 0.31 ± 0.08 times as high, respectively, as those in the control group ($p < 0.01$; Figure 4I–K; Figure S3H–K).

Effects of EHDPP on Placental Structure and Pregnancy in Female Mice

To investigate whether EHDPP can induce disruption of placentation *in vivo*, CD-1 mice were treated with EHDPP during pregestation period (2 wk) and gestation (Figure 5A). This study detected caudal-type homeobox 2 (Cdx2) and Ki67 in extra-embryonic ectoderm for E7.5 (late gastrulating embryos) fetuses (Figure 5B). We found that Ki67 and Cdx2 expression levels in the 10 mg/kg EHDPP exposure group were 0.88 ± 0.07 and 0.70 ± 0.22 times as high, respectively, as those in the control group ($p < 0.05$, Figure 5C–E). The structure of the E19.5 placentas in antepartum was also observed. The levels of trophoblast-specific protein α (TPBPA), transcription factor AP-2 γ (TFAP2C), and neural crest derivative-expressed protein 1 (HAND1) in the 10 mg/kg EHDPP exposure group were 0.88 ± 0.07, 0.88 ± 0.07, and 0.70 ± 0.22 times as high, respectively, as those in the control group ($p < 0.05$; Figure 5F,G; Figure S4A–D).

This study also analyzed IGF1R activity in mature placentas. The levels of p-IGF1R in the 0.4, 2, and 10 mg/kg EHDPP exposure groups were 0.53 ± 0.27, 0.48 ± 0.26, and 0.50 ± 0.20 times as high, respectively, as those in the control group ($p < 0.05$; Figure 5H; Figure S4E). These results were verified by immunofluorescence (Figure S4F). The levels of PD in the 0.4, 2, and 10 mg/kg EHDPP exposure groups were 0.80 ± 0.19, 0.68 ± 0.17 ($p < 0.05$), and 0.60 ± 0.16 ($p < 0.05$) times as high, respectively, as those in the control group (Figure 5H; Figure S4G). Cytochrome C participates in mitochondrial electron transport in aerobic respiration.[36] The levels of cytochrome C in the 0.4, 2, and 10 mg/kg EHDPP exposure groups were 0.83 ± 0.07 ($p < 0.05$), 0.75 ± 0.22, and 0.61 ± 0.20 ($p < 0.05$) times as high, respectively, as those in

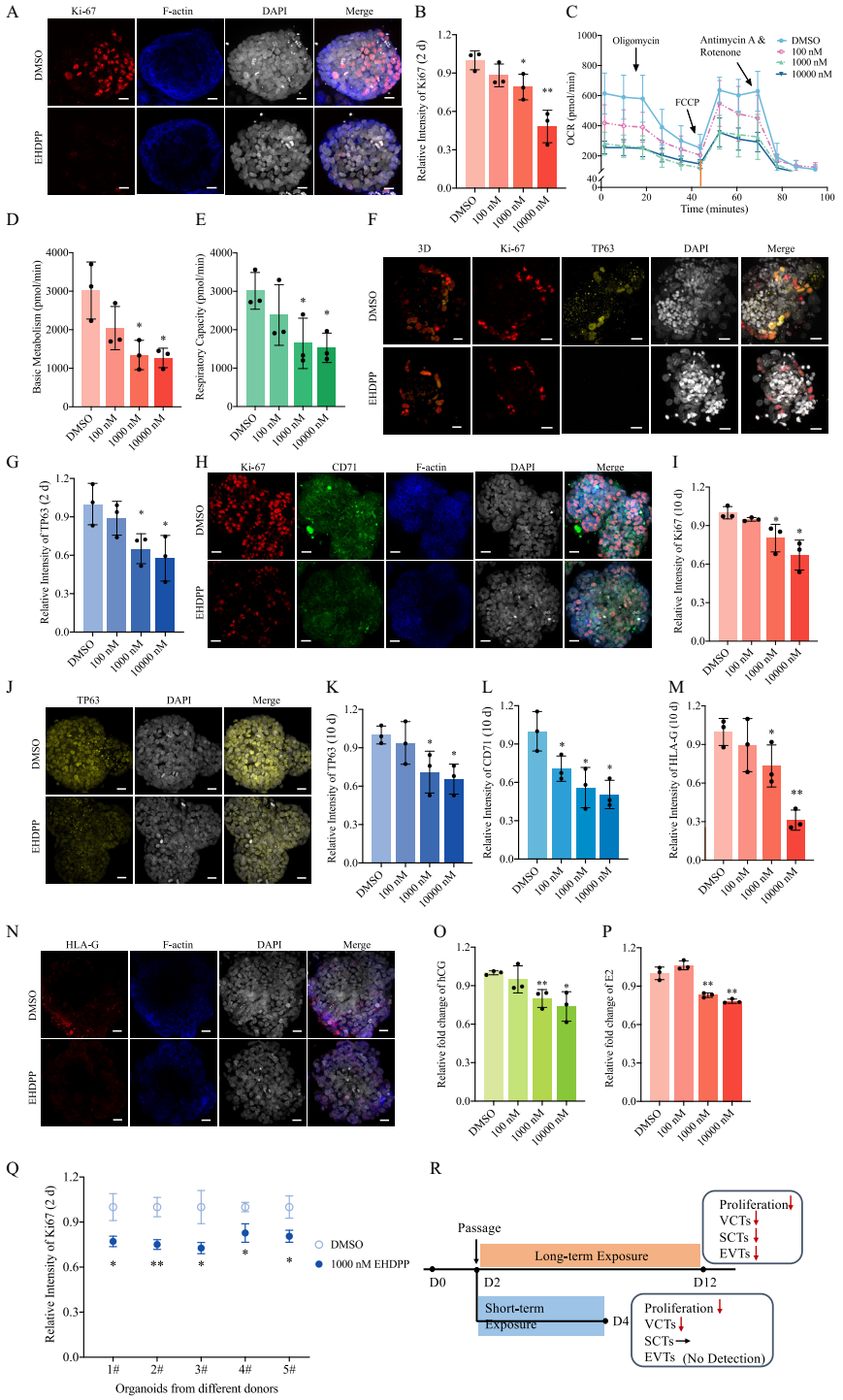

Figure 3. Measures of short- and long-term toxicity of EHDPP in organoids. (A) Ki67 (red), F-actin (blue) and DAPI (gray) in control and 2-d EHDPP (10,000 nM) exposure groups; (B) Relative intensity of Ki67 (means ± SDs) after 2-d EHDPP exposure; (C) Mitochondrial respirometry stress measurements by OCR (means ± SDs) in control and 2-d EHDPP (10,000 nM) exposure groups; (D) Basic metabolism (means ± SDs) in mitochondrial respirometry measurements calculated in (C); (E) Respiratory capacity (means ± SDs) in mitochondrial respirometry measurements calculated in (C); (F) Ki67 (red), TP63 (yellow), DAPI (gray) and 3D (three fluorescent light channel merged and remodeled by Imaris) in control and 2-d EHDPP (10,000 nM) exposure groups; (G)Relative intensity of TP63 (means ± SDs) after 2-d EHDPP exposure; (H) Ki67 (red), CD71 (green), F-actin (blue) and DAPI (gray) in control and 10-d EHDPP exposure groups; (I) Relative intensity of Ki67 (means ± SDs) after 10-d EHDPP exposure; (J) TP63 (yellow) and DAPI (gray) in control and 10-d EHDPP exposure groups; (K) Relative intensity of TP63 (means ± SDs) after 10-d EHDPP exposure; (L) Relative intensity of CD71 (means ± SDs) 10-d EHDPP exposure; (M) Relative intensity of HLA-G (means ± SDs) after 10-d EHDPP exposure; (N) HLA-G (red), F-actin (blue), and DAPI (gray) in control and 10-d EHDPP (10,000 nM) exposure groups; (O) Relative fold change of hCG (means ± SDs) after 10-d EHDPP exposure; (P) Relative fold change of E_2 (means ± SDs) 10-d EHDPP exposure;; (Q) Relative intensity of Ki67 (means ± SDs) after EHDPP exposure in organoids developed from five donors. (R) Summary of EHDPP-induced placentation disruption in trophoblast organoids. Data in (B), (G), (I), (K), (L), (M), (O), (P) are expressed relative to the levels in DMSO-treated organoids, which were set to 1. $n = 3$. All organoids in (Figure A–P) were from a single donor. Data were analyzed using an unpaired two-tailed Student's *t*-test. Indicated values are significantly different from the control value. Scale bars, 20 μm. Numeric data in (B), (D), (E), (G), (I), (K), (L), (M), (O) and (P) were listed in Table S9. Numeric data in (C) was listed in Table S10. Numeric data in (Q) was listed in Table S11. Note: CD71, transferrin receptor; E_2, estradiol; DMSO, dimethyl sulfoxide; DAPI, 4′,6-diamidino-2-phenylindole; EHDPP, 2-ethylhexyl-diphenyl phosphate; hCG, human chorionic gonadotropin; HLA-G, human leukocyte antigen protein-G; OCR, O_2 consumption rate; SD, standard deviation; TP63, tumor protein 63. $^{*}p < 0.05$. $^{**}p < 0.01$.

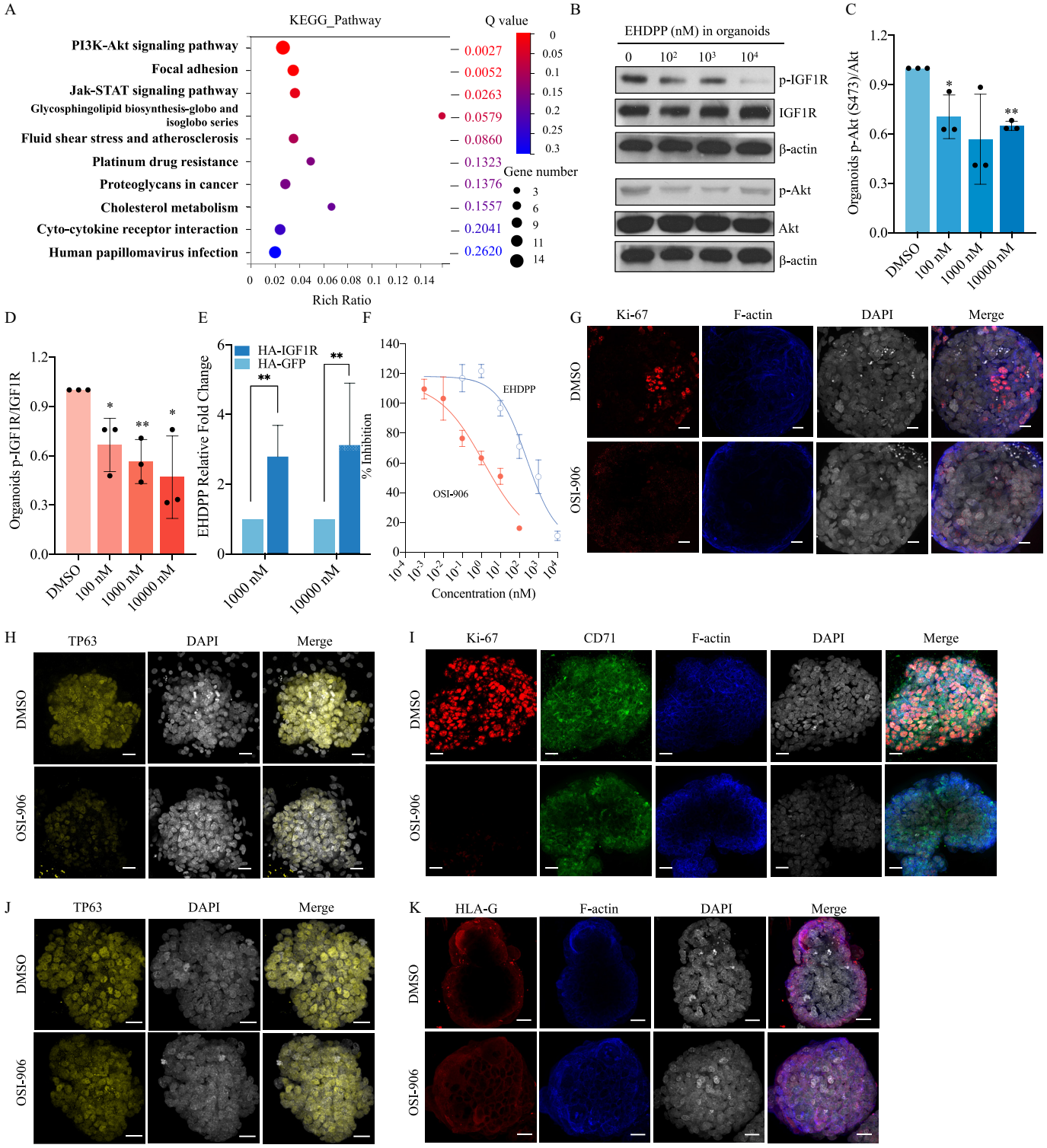

Figure 4. Investigating mechanisms of placentation disruption using organoids. (A) RNA-seq in Control and EHDPP (10,000 nM) exposure groups in trophoblast organoids; (B) Protein levels of p-IGF1R (Y1135), IGF1R, p-Akt (S473), Akt and β-actin in control and EHDPP exposure groups in trophoblast organoids; (C) Relative protein level (means ± SDs) of p-Akt (Ser_{473})/Akt; (D) Relative protein level (means ± SDs) of p-IGF1R/IGF1R; (E) Relative binding affinity of EHDPP (means ± SDs); (F) *In vitro* kinase activity (means ± SDs) of IGF1R of EHDPP and OSI-906 (50 nM); (G) Ki67 (red), F-actin (blue) and DAPI (gray) in control and 2-d OSI-906 (50 nM) exposure groups; (H) TP63 (yellow) and DAPI (gray) in control and 2-d OSI-906 (50 nM) exposure groups; (I) Ki67 (red), CD71 (green), F-actin (blue) and DAPI (gray) in control and 10-d OSI-906 (50 nM) exposure groups; (J) TP63 (red) and DAPI (gray) in control and 10-d OSI-906 (50 nM) exposure groups; (K) HLA-G (red), F-actin (blue) and DAPI (gray) in control and 10-d OSI-906 (50 nM) exposure groups. Data in (C–F) are expressed relative to the levels in DMSO-treated organoids, which were set to 1. $n = 3$. All organoids in Figure 4 were from a single donor. Data were analyzed using an unpaired two-tailed Student's *t*-test. Indicated values are significantly different from the control value. Scale bars, 20 μm. Numeric data in (C), (D) and (E) are listed in Table S12. Numeric data in (F) are listed in Table S13. Note: Akt, protein kinases B; CD71, transferrin receptor; DAPI, 4′,6-diamidino-2-phenylindole; DMSO, dimethylsulfoxide; EHDPP, 2-ethylhexyl-diphenyl phosphate; HLA-G, human leukocyte antigen protein-G; IGF1R, insulin-like growth factor 1 receptor; OSI-906, linsitinib; RNA-seq, RNA sequencing; SD, standard deviation; TP63, tumor protein 63. $^{*}p < 0.05$. $^{**}p < 0.01$.

the control group (Figure 5H; Figure S4H). Global transcript expression profiles in the 10 mg/kg EHDPP-treated E19.5 fetal placentas were evaluated by gene set enrichment analysis (GSEA). Several gene sets, including the oxidative phosphorylation gene set [normalized enrichment score (NES) = 1.76, $p < 0.01$], the tricarboxylic acid (TCA) cycle and respiratory electron transport gene set (NES = −1.89, $p < 0.01$), and the respiratory chain gene set (NES = −1.48, $p < 0.01$) (Figure 4I; Figure S4I), were found to be enriched in the control group relative to the 10 mg/kg EHDPP exposure group.

E19.5 fetal body weights in the 0.4, 2, and 10 mg/kg exposure groups were 1.490 ± 0.145 g, 1.429 ± 0.142 g, and 1.401 ± 0.146 g, respectively. The fetal BWs observed in the 2 and 10 mg/kg exposure groups were significantly lower than those in the control group (1.495 ± 0.105 g, $p < 0.01$) (Figure 5J). The comparative FGR incidence rates were found to be higher by 31% (50/159) and 38% (59/157) in the 2 and 10 mg/kg EHDPP exposure groups, respectively ($p < 0.01$) (Figure S4J). The results of an OGTT in 8-wk-old offspring indicated significantly impaired glucose tolerance in the groups exposed to 2 and 10 mg/kg relative to the control group (Figure 5K).

In the 0.4-, 2-, and 10-mg/kg EHDPP exposure groups, the relative numbers of implanted embryos were 0.97 ± 0.13, 0.91 ± 0.13, and 0.88 ± 0.11 ($p < 0.05$) times as high, respectively, as those in the control group (Figure 5L). The relative numbers of surviving embryos in the 0.4, 2, and 10 mg/kg EHDPP exposure groups were 0.94 ± 0.11, 0.84 ± 0.17 ($p < 0.05$), and 0.81 ± 0.18 ($p < 0.05$) times as high, respectively, as those in the control group (Figure 5M). Stillbirth in the EHDPP exposure groups was demonstrated by the recorded resorption and stillborn fetuses (Figure 5N).

The average concentration of EHDPP in E19.5 placentas from the 10 mg/kg EHDPP exposure group was 0.495 ± 0.261 ng/g dw.

Discussion

A meta-analysis has indicated an increasing incidence of pathological placentation in recent years,[37] and the initiation and progression of placental disorders may be driven by environmental factors. The production of OPFRs is increasing and thus exposure is increasing, especially exposure via indoor dust, due to their widespread application in furniture and electronics and even in food packing materials. OPFRs that have been not adequately tested for human toxicity were and are currently allowed on the market.[38] To model this scenario, we devised a screening model based on human trophoblast organoids with visual readout to screen 46 OPFRs. To evaluate the toxicity of chemicals in a time- and cost-efficient manner, we optimized the original organoid culture method by reducing the digestion level so that the organoids were larger and we increased the concentration of molecules that can promote proliferation. In an approach similar to organoids derived using a previously described protocol,[23] GATA-3 and KRT7, which are markers of trophoblast organoids,

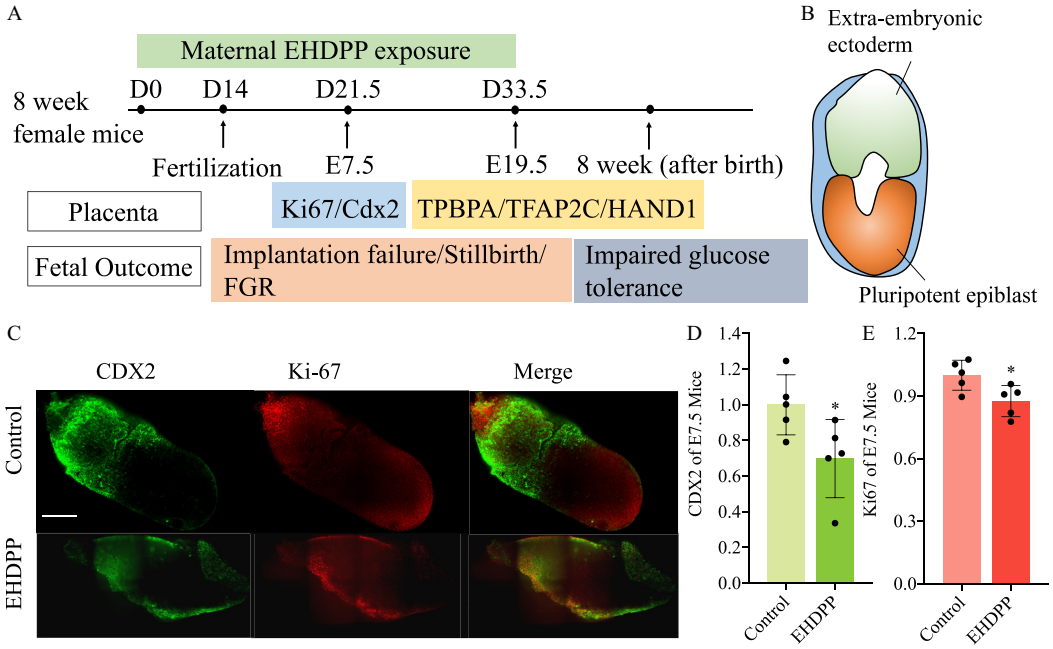

Figure 5. Effects of EHDPP on placental structure and pregnancy in female mice. (A) CD-1 female mice exposed to EHDPP; (B) Schematic of E7.5 embryo; (C) Cdx2 (green), Ki67, and DAPI (blue) in E7.5 in control and EHDPP (10 mg/kg/d) exposure groups ($n = 5$) (Scale bars, 20 μm); (D) Relative intensity of Cdx2 (means ± SDs) in control and EHDPP (10 mg/kg/d) exposure groups; (E) Relative intensity of Ki67 (means ± SDs) in control and EHDPP (10 mg/kg/d) exposure groups; (F) TPBPA (red) and DAPI (blue) in E19.5 placentas in control and EHDPP (10 mg/kg/d) exposure groups; (G) TFAP2C (red) and DAPI (blue) in E19.5 placentas in control and EHDPP (10 mg/kg/d) exposure groups ($n = 5$); (H) Protein levels of p-IGF1R (Y1135), IGF1R, PD, Cytochrome C and β-actin in E19.5 fetal placentas treated with EHDPP; (I) GSEA analysis between placentas of control and 10 mg/kg EHDPP exposure group; (J) E19.5 fetal weight (means ± SDs) after EHDPP exposure to pregnant mouse; (K) OGTT in 4-wk-old offspring after intrauterine EHDPP exposure (blood glucose concentrations; means ± SDs); (L) Survived embryonic numbers (means ± SDs) in control and EHDPP exposure groups; (M) Implanted embryonic numbers (means ± SDs) in control and EHDPP exposure groups; (N) Resorption and stillborn after EHDPP exposure. Data in (D) and (E) and (L) and (M) are expressed relative to the levels in the control group, which were set to 1. (C–G), $n = 5$; (H) and (I), $n = 3$; (K), five female and five male offspring; (J), (L–N), $n = 10$. Data were analyzed using an unpaired two-tailed Student's t-test. Indicated values are significantly different from the control value. (F–G): Scale bars: 500 μm in ×2 and 50 μm in ×40. Numeric data in (D), (E), (J), (L) and (M) are listed in Table S14. Numeric data in (K) are listed in Table S15. Note: Cdx2, caudal-type homeobox 2; DAPI, 4′,6-diamidino-2-phenylindole; E7.5, late gastrulation stage embryos; E19.5, newborn mouse; EHDPP, 2-ethylhexyl-diphenyl phosphate; GSEA, gene set enrichment analysis; IGF1R, insulin-like growth factor 1 receptor; OGTT, oral glucose tolerance test; PD, pyruvate dehydrogenase complex; SD, standard deviation; TFAP2C, transcription factor AP-2γ; TPBPA, trophoblast-specific protein α. $^{*}p < 0.05$ and $^{**}p < 0.01$.

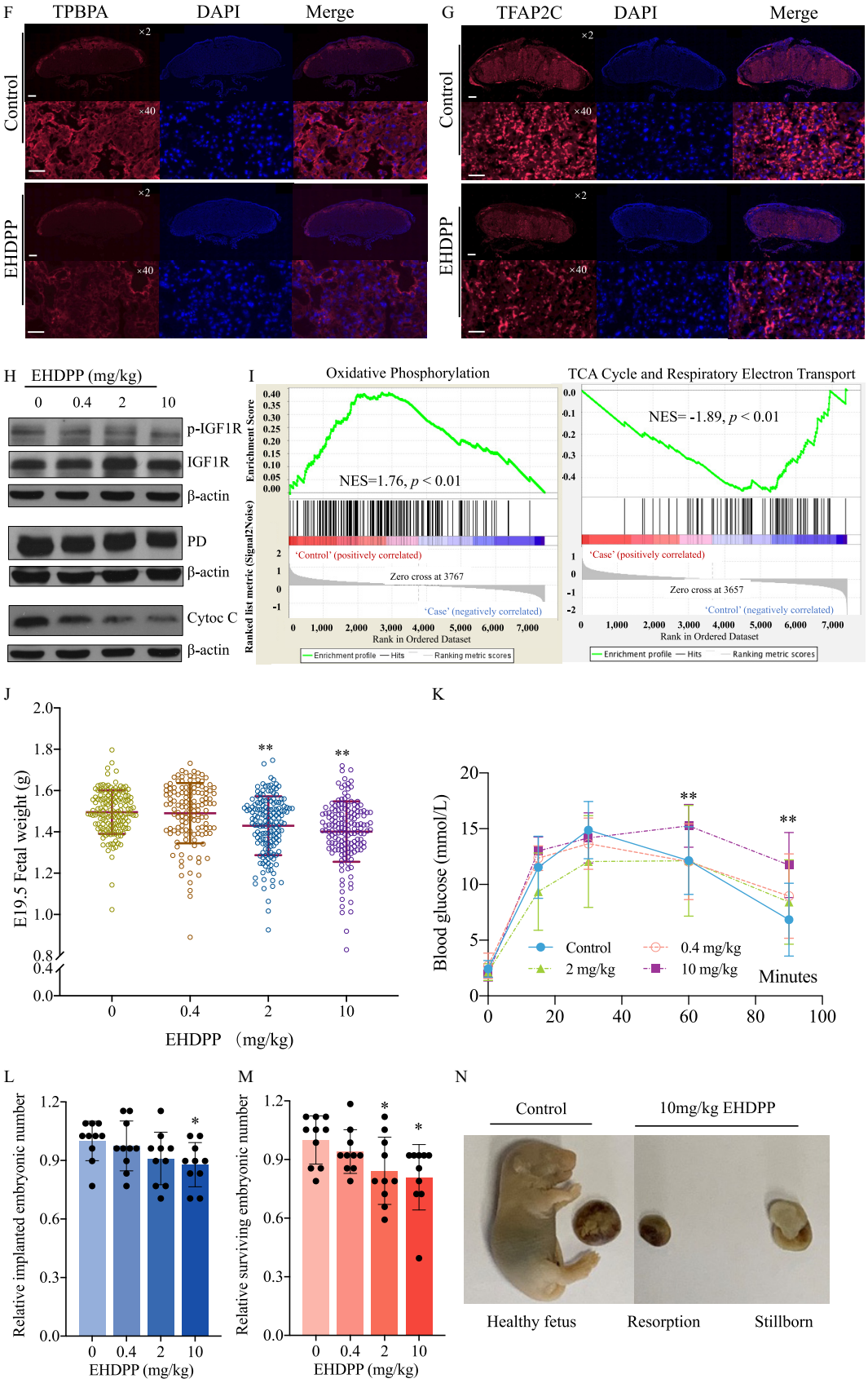

Figure 5. (*Continued.*)

and hCG were detected in organoids derived from the optimized protocol described herein. Proliferation is critical to maintain the self-renewal and the normal structure and function of a developing placenta.[14] Once a chemical inhibits the proliferative capacity of a human trophoblast organoid, it hinders the process of trophoblast differentiation, which has the potential to induce a placentation disorder. Among OPFRs, three aryl-OPFRs (EHDPP, o-TCrP, and B4tBPPP) were identified to inhibit the proliferation of human trophoblast organoids.

Of the three identified OPFRs, EHDPP has been widely detected in environmental samples, including soil,[21] floor dust,[39] drinking water,[40] and food.[41] Moreover, EHDPP is the only organophosphate ester approved by the U.S. Food and Drug Administration Center for Food Safety and Applied Nutrition for use as a fire retardant in food packaging materials.[42] Because EHDPP has been detected in human blood,[22] deciduae, and villi,[20] its effects on pregnancy outcomes require further investigation. Further analysis established that a 2-d exposure to EHDPP significantly inhibited proliferation of organoids, and the combination of these results (lower basic metabolism, respiratory capacity, and PD protein level) together suggested that the tricarboxylic acid cycle was impaired by EHDPP. Proliferating cells in trophoblast organoids require the tricarboxylic acid cycle to maintain an open chromatin state.[43] VCTs are the main proliferating cells in the human placenta,[14] the lower VCT count suggested that the disruption of proliferation by EHDPP may mainly represent the inhibition of VCT proliferation in trophoblast organoids. VCTs differentiate into SCTs and EVTs.[14] No significant difference in SCTs after 2-d EHDPP exposure and the lower number of SCTs after 10-d exposure suggested the exhaustion of VCTs may impact SCTs. Because SCTs secrete hormones, such as E_2 and hCG,[14] the low number of SCTs after 10 d of exposure to EHDPP may have led to lower E_2 and hCG levels than those in the control group, indicating the dysfunction of trophoblast organoids. The role of EVTs is to anchor the placenta to the uterus and transform the maternal spiral arteries to increase blood flow by invasion,[44] and thus the lower number of EVTs suggested that EHDPP may impair invasion. The similar inhibition of proliferation was also observed in the other four strains of organoids, suggesting that EHDPP may have a specific mechanism that is not only effective in sensitive individual. The concentration of EHDPP after 2-d EHDPP exposure was comparable with that in human villi (873 ng/g dw),[20] showing our results have environmental significance.

Placentation disorder is a complicated and systemic process in mammals,[14] and causative connections between environmental factors and specific targets during placentation are indistinct. Using RNA-seq, the PI3K-Akt pathway was found to be significantly enriched after EHDPP exposure in organoids, with a lower Q value and a greater number of enriched genes than the other pathways based on KEGG analysis. Lower p-Akt (Ser473) levels in the exposure groups than in the control group confirmed the inhibition of Akt in organoids, because the phosphorylation of Ser473 in Akt indicates its full activation.[45] Because Akt regulates cell proliferation in the placenta,[45] the inhibition of proliferation observed in this study may be attributed to the inhibition of Akt. IGF1 and IGF2 are powerful mitogens in the first trimester of pregnancy that act via IGF1R, which regulates the activation of the PI3K-Akt pathway in mammals.[46,47] The inhibition of IGF1R in organoids exposed to EHDPP and the structural disorder of trophoblast organoids exposed to OSI-906 (a specific antagonist of IGF1R)[48] suggested that IGF1R plays a key role in EHDPP-induced structural disorders of trophoblast organoids. The inhibition of IGF1R activity may result from low expression levels of IGFs or the inhibition of the intracellular kinase domain of IGF1R.[49,50] We found that EHDPP binds to IGF1R and inhibits its kinase activity *in vitro*. Although the IC_{50} value of EHDPP was higher than that of OSI-906, the strong IGF1R-antigonistic activity of EHDPP was unexpected, as it is an industrial chemical that was not designed as a drug. Because no significant down-regulation in IGF1 or IGF2 expression levels were observed in organoids, EHDPP may antagonize IGF1R activity by directly binding to IGF1R, leading to the placentation disorder in human trophoblast organoids. Additionally, organoids exposed to EHDPP actually showed higher levels of IGF2, which might be feedback regulation because the IGF1R of high activity is crucial in human placentation.[14] However, we cannot fully exclude other latent pathways.

Extending these results to similar susceptibility *in vivo*, mice exposed to EHDPP were also found to exhibit structure disorder and impaired aerobic respiration in the placenta. Late gastrulation (E7.5) is a critical stage in placentation in mice.[51] Cdx2 is a marker of extra-embryonic ectoderm in E7.5 mouse fetuses and controls the proliferation and differentiation of extra-embryonic ectoderm.[52,53] The lower Cdx2 and Ki67 expressions in placentas of mice exposed to EHDPP than in the control suggested that EHDPP inhibited proliferation and disrupted extra-embryonic ectoderm in mice. Extra-embryonic ectoderm in the immature placenta can differentiate to spongiotrophoblast (SP) and trophoblast giant cells (TGC) in mice.[51] SPs were identified by TPBPA and TFAP2C expression and TGCs were identified by HAND1 and TFAP2C expression in the placentas of E19.5 mice. Lower TPBPA, TFAP2C, and HAND1 levels observed in the exposure groups in comparison with the control group suggested that the SPs and TGCs were disrupted by EHDPP. Because SPs and TGCs secrete hormones and cytokines and exchange materials between the maternal bloodstream and the fetus,[51] EHDPP may affect the function of mature placentas in mice. The lower levels of p-IGF1R protein and aerobic respiration disorder observed in E19.5 placentas suggested that similar mechanism in exposure to EHDPP in trophoblast organoids occurred *in vivo*. In EHDPP exposure groups, we observed implantation failure, stillbirth, FGR of fetuses, and impaired glucose tolerance in adulthood after birth. These outcomes are regulated by many developmental processes during pregnancy in humans and mice, such as maternal endocrine factors and deficient spiral artery remodeling of the placenta[54] and could not be fully evaluated in this study. Adverse pregnancy outcomes such as stillbirth,[55] implantation failure,[56] and FGR[57] may have placental origins, and some studies have found that adult metabolic disorders may be influenced by placental insufficiency.[58,59] EHDPP-induced placentation disorder provided a possible explanation for the occurrences of these pathological phenomena. The EHDPP concentration detected in placentas from the group of mice exposed to the highest concentration was lower than the median EHDPP concentration in human deciduae (5.96 ng/g of dw) and chorionic villi (13.6 ng/g of dw).[20] Thus, adverse pregnancy outcomes and impaired glucose tolerance in offspring may occur at physiological human concentrations of EHDPP, posing notable risks to gestation and of lifelong metabolic disease in humans. Although the association of EHDPP with these diseases in humans is unclear, epidemiological studies have associated a common metabolite of several aryl-OPFRs including EHDPP with low birth weight[60] and decreased success of fertilization, implantation, and clinical pregnancy.[18] The results of this study suggest a causal relationship between EHDPP exposure and adverse pregnancy outcomes in mice, as supported by primary trophoblast organoid culture data.

In summary, the present study clarified the adverse effects of a commonly used flame retardant EHDPP on human placentation by devising a model based on human trophoblast organoids. The adverse effects of EHDPP on placentation were demonstrated in

mice, where it induced fetal growth restriction, implantation failure, stillbirth, and impaired glucose tolerance at physiological human concentrations. Human pregnancy is a long-term life process. Our study may provide prospective and mechanistic insights into the potential correlations between early-life exposure to EHDPP and adverse pregnancy outcomes in humans and a potential approach to high-throughput screen these chemicals in future chemical management. A limitation of this paper is that all structural disorders and dysfunctions induced by EHDPP were observed in the same strain of organoids from one donor, whereas there are interindividual differences, such as the difference in the epigenetic modification level of trophoblast organoids, which may be influenced by various factors, including fetal sex, karyotype, gestational age, and even the maternal health. This study could not give more information about interindividual differences in toxicity of EHDPP exposure because relatively large samples are required but difficult to obtain. However, this toxicity model based on human trophoblast organoids may be helpful to fill the gap in how interindividual differences play their roles in early-life exposure to contamination, and such knowledge may benefit sensitive individuals in the future.

Acknowledgments

The authors thank S. Qin at the Core Facilities of the School of Life Sciences and H. Lv, G. Li, and H. Yang at National Center for Protein Sciences at Peking University in Beijing, China.

This study received financial support from the National Natural Science Foundation of China (21737001, 22076005, and 41821005).

C.X. and J.H. designed the study. F.G. performed the collection of human samples. C.X., H.M., C.Z., J.X., and Y.J. performed the experiments and collected data. C.X., F.G., and J.H. analyzed the data. C.X., W.H., J.X., and J.H. wrote the manuscript.

References

1. U.S. Centers for Disease Control and Prevention (CDC). 2019. Data on Selected Pregnancy Complications in the United States. https://www.cdc.gov/reproductivehealth/maternalinfanthealth/pregnancy-complications-data.htm#hyper [accessed 20 April 2022].
2. Organization for Economic Cooperation and Development (OECD). 2021. Infant mortality, OECD Health Statistics 2021 Definitions, Sources and Methods. https://stats.oecd.org/index.aspx [accessed 20 April 2022].
3. Pearson-Stuttard J, Buckley J, Cicek M, Gregg EW. 2021. The changing nature of mortality and morbidity in patients with diabetes. Endocrinol Metab Clin North Am 50(3):357–368, PMID: 34399950, https://doi.org/10.1016/j.ecl.2021.05.001.
4. Woodruff TJ, Janssen SJ, Guillette Jr LJ. 2010. *Environmental Impacts on Reproductive Health and Fertility*. Cambridge, UK: Cambridge University Press. https://doi.org/10.1017/CBO9780511674686.
5. Di Renzo GC, Conry JA, Blake J, DeFrancesco MS, DeNicola N, Martin JN, et al. 2015. International federation of gynecology and obstetrics opinion on reproductive health impacts of exposure to toxic environmental chemicals. Int J Gynaecol Obstet 131(3):219–225, PMID: 26433469, https://doi.org/10.1016/j.ijgo.2015.09.002.
6. Bergman Å, Heindel J, Jobling S, Kidd K, Zoeller RT. 2012. State-of-the-science of endocrine disrupting chemicals, 2012. Toxicol Lett 211 (suppl):S3, https://doi.org/10.1016/j.toxlet.2012.03.020.
7. Trasande L, Shaffer RM, Sathyanarayana S, Lowry JA, Ahdoot S, Baum CR, et al. 2018. Food additives and child health. Pediatrics 142(2):e20181410, PMID: 30037972, https://doi.org/10.1542/peds.2018-1410.
8. Trasande L, Zoeller RT, Hass U, Kortenkamp A, Grandjean P, Myers JP, et al. 2016. Burden of disease and costs of exposure to endocrine disrupting chemicals in the European Union: an updated analysis. Andrology 4(4):565–572, PMID: 27003928, https://doi.org/10.1111/andr.12178.
9. Trasande L, Zoeller RT, Hass U, Kortenkamp A, Grandjean P, Myers JP, et al. 2015. Estimating burden and disease costs of exposure to endocrine-disrupting chemicals in the European Union. J Clin Endocrinol Metab 100(4):1245–1255, PMID: 25742516, https://doi.org/10.1210/jc.2014-4324.
10. Kahn LG, Philippat C, Nakayama SF, Slama R, Trasande L. 2020. Endocrine-disrupting chemicals: implications for human health. Lancet Diabetes Endocrinol 8(8):703–718, PMID: 32707118, https://doi.org/10.1016/S2213-8587(20)30129-7.
11. Kamai E, McElrath T, Ferguson K. 2019. Fetal growth in environmental epidemiology: mechanisms, limitations, and a review of associations with biomarkers of non-persistent chemical exposures during pregnancy. Environ Health 18(1):43, PMID: 31068204, https://doi.org/10.1186/s12940-019-0480-8.
12. Ilekis JV, Tsilou E, Fisher S, Abrahams VM, Soares MJ, Cross JC, et al. 2016. Placental origins of adverse pregnancy outcomes: potential molecular targets: an Executive Workshop Summary of the *Eunice Kennedy Shriver* National Institute of Child Health and Human Development. Am J Obstet Gynecol 215(1 suppl):S1–S46, PMID: 26972897, https://doi.org/10.1016/j.ajog.2016.03.001.
13. Gingrich J, Ticiani E, Veiga-Lopez A. 2020. Placenta disrupted: endocrine disrupting chemicals and pregnancy. Trends Endocrinol Metab 31(7):508–524, PMID: 32249015, https://doi.org/10.1016/j.tem.2020.03.003.
14. Benirschke K, Burton GJ, Baergen RN. 2012. *Pathology of the Human Placenta. 6th* ed. New York, NY: Springer.
15. Houck K, Dix D, Judson R, Kavlock R, Yang J, Berg E. 2009. Profiling bioactivity of the ToxCast chemical library using BioMAP primary human cell systems. J Biomol Screen 14(9):1054–1066, PMID: 19773588, https://doi.org/10.1177/1087057109345525.
16. Kleinstreuer NC, Yang J, Berg EL, Knudsen TB, Richard AM, Martin MT, et al. 2014. Phenotypic screening of the ToxCast chemical library to classify toxic and therapeutic mechanisms. Nat Biotechnol 32(6):583–591, PMID: 24837663, https://doi.org/10.1038/nbt.2914.
17. Turco MY, Gardner L, Kay RG, Hamilton RS, Prater M, Hollinshead MS, et al. 2018. Trophoblast organoids as a model for maternal-fetal interactions during human placentation. Nature 564(7735):263–267, PMID: 30487605, https://doi.org/10.1038/s41586-018-0753-3.
18. Carignan CC, Alarcón LM, Butt CM, Williams PL, Meeker JD, Stapleton HM, et al. EARTH Study Team. 2017. Urinary concentrations of organophosphate flame retardant metabolites and pregnancy outcomes among women undergoing *in vitro* fertilization. Environ Health Perspect 125(8):087018, PMID: 28858831, https://doi.org/10.1289/EHP1021.
19. Chupeau Z, Bonvallot N, Mercier F, Le Bot B, Chevrier C, Glorennec P. 2020. Organophosphorus flame retardants: a global review of indoor contamination and human exposure in Europe and epidemiological evidence. Int J Environ Res Public Health 17(18):6713, PMID: 32942622, https://doi.org/10.3390/ijerph17186713.
20. Zhao F, Chen M, Gao F, Shen H, Hu J. 2017. Organophosphorus flame retardants in pregnant women and their transfer to chorionic villi. Environ Sci Technol 51(11):6489–6497, PMID: 28516762, https://doi.org/10.1021/acs.est.7b01122.
21. Ji Y, Wang Y, Yao Y, Ren C, Lan Z, Fang X, et al. 2019. Occurrence of organophosphate flame retardants in farmland soils from Northern China: primary source analysis and risk assessment. Environ Pollut 247:832–838, PMID: 30731308, https://doi.org/10.1016/j.envpol.2019.01.036.
22. Zhao F, Li Y, Zhang S, Ding M, Hu J. 2019. Association of aryl organophosphate flame retardants triphenyl phosphate and 2-ethylhexyl diphenyl phosphate with human blood triglyceride and total cholesterol levels. Environ Sci Technol Lett 6(9):532–537, https://doi.org/10.1021/acs.estlett.9b00417.
23. Sheridan MA, Fernando RC, Gardner L, Hollinshead MS, Burton GJ, Moffett A, et al. 2020. Establishment and differentiation of long-term trophoblast organoid cultures from the human placenta. Nat Protoc 15(10):3441–3463, PMID: 32908314, https://doi.org/10.1038/s41596-020-0381-x.
24. Pachenari N, Kiani S, Javan M. 2017. Inhibition of glycogen synthase kinase 3 increased subventricular zone stem cells proliferation. Biomed Pharmacother 93:1074–1082, PMID: 28738501, https://doi.org/10.1016/j.biopha.2017.07.043.
25. Wang T, Kang W, Du L, Ge S. 2017. Rho-kinase inhibitor Y-27632 facilitates the proliferation, migration and pluripotency of human periodontal ligament stem cells. J Cell Mol Med 21(11):3100–3112, PMID: 28661039, https://doi.org/10.1111/jcmm.13222.
26. Li S, Sun Z, Zhang Y, Ruan Y, Chen Q, Gong W, et al. 2017. COX-2/mPGES-1/PGE_2 cascade activation mediates uric acid-induced mesangial cell proliferation. Oncotarget 8(6):10185–10198, PMID: 28052039, https://doi.org/10.18632/oncotarget.14363.
27. Thakur S, Cattoni DI, Nöllmann M. 2015. The fluorescence properties and binding mechanism of SYTOX green, a bright, low photo-damage DNA intercalating agent. Eur Biophys J 44(5):337–348, PMID: 26024786, https://doi.org/10.1007/s00249-015-1027-8.
28. Hu W, Gao F, Zhang H, Hiromori Y, Arakawa S, Nagase H, et al. 2017. Activation of peroxisome Proliferator-Activated receptor gamma and disruption of progesterone synthesis of 2-ethylhexyl diphenyl phosphate in human placental choriocarcinoma cells: comparison with triphenyl phosphate. Environ Sci Technol 51(7):4061–4068, PMID: 28282128, https://doi.org/10.1021/acs.est.7b00872.
29. Schindelin J, Arganda-Carreras I, Frise E, Kaynig V, Longair M, Pietzsch T, et al. 2012. Fiji: an open-source platform for biological-image analysis. Nat Methods 9(7):676–682, PMID: 22743772, https://doi.org/10.1038/nmeth.
30. Noyola-Martínez N, Halhali A, Barrera D. 2019. Steroid hormones and pregnancy. Gynecol Endocrinol 35(5):376–384, PMID: 30793997, https://doi.org/10.1080/09513590.2018.1564742.

31. Cock PJ, Fields CJ, Goto N, Heuer ML, Rice PM. 2010. The Sanger FASTQ file format for sequences with quality scores, and the Solexa/Illumina FASTQ variants. Nucleic Acids Res 38(6):1767–1771, PMID: 20015970, https://doi.org/10.1093/nar/gkp1137.
32. Kim D, Langmead B, Salzberg SL. 2015. HISAT: a fast spliced aligner with low memory requirements. Nat Methods 12(4):357–360, PMID: 25751142, https://doi.org/10.1038/nmeth.3317.
33. Langmead B, Trapnell C, Pop M, Salzberg SL. 2009. Ultrafast and memory-efficient alignment of short DNA sequences to the human genome. Genome Biol 10(3):R25, PMID: 19261174, https://doi.org/10.1186/gb-2009-10-3-r25.
34. Devaskar SU, Chu A. 2016. Intrauterine growth restriction: hungry for an answer. Physiology (Bethesda) 31(2):131–146, PMID: 26889018, https://doi.org/10.1152/physiol.00033.2015.
35. Shea K, Geijsen N. 2007. Dissection of 6.5 dpc mouse embryos. J Vis Exp (2):160, PMID: 18830421, https://doi.org/10.3791/160.
36. Timón-Gómez A, Nývltová E, Abriata LA, Vila AJ, Hosler J, Barrientos A. 2018. Mitochondrial cytochrome c oxidase biogenesis: recent developments. Semin Cell Dev Biol 76:163–178, PMID: 28870773, https://doi.org/10.1016/j.semcdb.2017.08.055.
37. Papanikolaou IG, Domali E, Daskalakis G, Theodora M, Telaki E, Drakakis P, et al. 2018. Abnormal placentation: current evidence and review of the literature. Eur J Obstet Gynecol Reprod Biol 228:98–105, PMID: 29913334, https://doi.org/10.1016/j.ejogrb.2018.06.004.
38. de Boer J, Stapleton HM. 2019. Toward fire safety without chemical risk. Science 364(6437):231–232, PMID: 31000649, https://doi.org/10.1126/science.aax2054.
39. Hu W, Jia Y, Kang Q, Peng H, Ma H, Zhang S, et al. 2019. Screening of house dust from chinese homes for chemicals with liver X receptors binding activities and characterization of atherosclerotic activity using an *in vitro* macrophage cell line and ApoE$^{-/-}$ mice. Environ Health Perspect 127(11):117003, PMID: 31724879, https://doi.org/10.1289/EHP5039.
40. Ji Y, Yu N, Zhang B, Jin L, Li M, Hu M, et al. 2014. Occurrence of organophosphate flame retardants in drinking water from China. Water Res 54:53–61, PMID: 24556230, https://doi.org/10.1016/j.watres.2014.01.031.
41. Zhao L, Jian K, Su H, Zhang Y, Li J, Letcher RJ, et al. 2019. Organophosphate esters (OPEs) in Chinese foodstuffs: dietary intake estimation via a market basket method, and suspect screening using high-resolution mass spectrometry. Environ Int 128:343–352, PMID: 31078003, https://doi.org/10.1016/j.envint.2019.04.055.
42. U.S. Food and Drug Administration. Inventory of Food Contact Substances Listed in 21 CFR: Diphenyl-2-Ethylhexyl Phosphate. https://www.cfsanappsexternal.fda.gov/scripts/fdcc/index.cfm?set=IndirectAdditives&id=DIPHENYLETHYLHEXYLPHOSPHATE [accessed 20 April 2022].
43. Mathieu J, Ruohola-Baker H. 2017. Metabolic remodeling during the loss and acquisition of pluripotency. Development 144(4):541–551, PMID: 28196802, https://doi.org/10.1242/dev.128389.
44. Hamilton WJ, Boyd JD. 1960. Development of the human placenta in the first three months of gestation. J Anat 94(Part 3):297–328. https://www.ncbi.nlm.nih.gov/pmc/articles/PMC1244370/pdf/janat00441-0002.pdf, PMID: 14399291.
45. Robey RB, Hay N. 2009. Is Akt the "Warburg kinase"?-Akt-energy metabolism interactions and oncogenesis. Semin Cancer Biol 19(1):25–31, PMID: 19130886, https://doi.org/10.1016/j.semcancer.2008.11.010.
46. Yang ZZ, Tschopp O, Hemmings-Mieszczak M, Feng J, Brodbeck D, Perentes E, et al. 2003. Protein kinase Bα/Akt1 regulates placental development and fetal growth. J Biol Chem 278(34):32124–32131, PMID: 12783884, https://doi.org/10.1074/jbc.M302847200.
47. Forbes K, Westwood M, Baker PN, Aplin JD. 2008. Insulin-like growth factor 1 and II regulate the life cycle of trophoblast in the developing human placenta. Am J Physiol Cell Physiol 294(6):1313–1322, PMID: 18400990, https://doi.org/10.1152/ajpcell.00035.2008.
48. Mulvihill MJ, Cooke A, Rosenfeld-Franklin M, Buck E, Foreman K, Landfair D, et al. 2009. Discovery of OSI-906: a selective and orally efficacious dual inhibitor of the IGF-1 receptor and insulin receptor. Future Med Chem 1(6):1153–1171, PMID: 21425998, https://doi.org/10.4155/fmc.09.89.
49. Holly J, Perks CM, Stewart C. 2000. Overview of insulin-like growth factor physiology. Growth Horm IGF Res 10 Suppl A:S8–9, PMID: 10984272, https://doi.org/10.1016/S1096-6374(00)90003-0.
50. Favelyukis S, Till JH, Hubbard SR, Miller WT. 2001. Structure and autoregulation of the insulin-like growth factor 1 receptor kinase. Nat Struct Biol 8(12):1058–1063, PMID: 11694888, https://doi.org/10.1038/nsb721.
51. Rossant J, Cross JC. 2001. Placental development: lessons from mouse mutants. Nat Rev Genet 2(7):538–548, PMID: 11433360, https://doi.org/10.1038/35080570.
52. Bergsmedh A, Donohoe ME, Hugh RA, Hadjantonakis AK. 2011. Understanding the molecular circuitry of cell lineage specification in the early mouse embryo. Genes (Basel) 2(3):420–448, PMID: 24710206, https://doi.org/10.3390/genes2030420.
53. Cross JC. 2005. How to make a placenta: mechanisms of trophoblast cell differentiation in mice – a review. Placenta 26 (suppl A):S3–S9, PMID: 15837063, https://doi.org/10.1016/j.placenta.2005.01.015.
54. Brosens I, Pijnenborg R, Vercruysse L, Romero R. 2011. The "great obstetrical syndromes" are associated with disorders of deep placentation. Am J Obstet Gynecol 204(3):193–201, PMID: 21094932, https://doi.org/10.1016/j.ajog.2010.08.009.
55. Graham N, Heazell AEP. 2020. When the fetus goes still and the birth is tragic: the role of the placenta in stillbirths. Obstet Gynecol Clin North Am 47(1):183–196, PMID: 32008668, https://doi.org/10.1016/j.ogc.2019.10.005.
56. Cross J, Werb Z, Fisher S. 1994. Implantation and the placenta: key pieces of the development puzzle. Science 266(5190):1508–1518, PMID: 7985020, https://doi.org/10.1126/science.7985020.
57. Chaddha V, Viero S, Huppertz B, Kingdom J. 2004. Developmental biology of the placenta and the origins of placental insufficiency. Semin Fetal Neonatal Med 9(5):357–369, PMID: 15691771, https://doi.org/10.1016/j.siny.2004.03.006.
58. Hales C, Barker D, Barber D. 2001. The thrifty phenotype hypothesis. Br Med Bull 60:5–20, PMID: 11809615, https://doi.org/10.1093/bmb/60.1.5.
59. Burton GJ, Fowden AL, Thornburg KL. 2016. Placental origins of chronic disease. Physiol Rev 96(4):1509–1565, PMID: 27604528, https://doi.org/10.1152/physrev.00029.2015.
60. Luo D, Liu W, Wu W, Tao Y, Hu L, Wang L, et al. 2021. Trimester-specific effects of maternal exposure to organophosphate flame retardants on offspring size at birth: a prospective cohort study in China. J Hazard Mater 406:124754, PMID: 33310325, https://doi.org/10.1016/j.jhazmat.2020.124754.